Effect of CoFe insertion in Co2MnSi/CoFe/n-GaAs junctions on spin injection properties

Yuya Ebina, Takafumi Akiho, Hong-xi Liu, Masafumi Yamamoto, and Tetsuya Uemura

Citation: Applied Physics Letters **104**, 172405 (2014); doi: 10.1063/1.4873720
View online: http://dx.doi.org/10.1063/1.4873720
View Table of Contents: http://scitation.aip.org/content/aip/journal/apl/104/17?ver=pdfcov
Published by the AIP Publishing

Effect of CoFe insertion in Co_2MnSi/CoFe/*n*-GaAs junctions on spin injection properties

Yuya Ebina, Takafumi Akiho, Hong-xi Liu, Masafumi Yamamoto, and Tetsuya Uemura[a)]
Division of Electronics for Informatics, Graduate School of Information Science and Technology, Hokkaido University, Sapporo 060-0814, Japan

(Received 26 February 2014; accepted 17 April 2014; published online 1 May 2014)

The CoFe thickness (t_{CoFe}) dependence of spin injection efficiency was investigated for Co_2MnSi/CoFe/*n*-GaAs junctions. The $\Delta V_{NL}/I$ value, which is a measure of spin injection efficiency, strongly depended on t_{CoFe}, where ΔV_{NL} is the amplitude of a nonlocal spin-valve signal, and I is an injection current. Importantly, the maximum value of $\Delta V_{NL}/I$ for a Co_2MnSi/CoFe/*n*-GaAs junction was one order of magnitude higher than that for a CoFe/*n*-GaAs junction, indicating that a Co_2MnSi electrode works as a highly polarized spin source. No clear spin signal, on the other hand, was observed for a Co_2MnSi/*n*-GaAs junction due to diffusion of Mn atoms into the GaAs channel. Secondary ion mass spectrometry analysis indicated that the CoFe insertion effectively suppressed the diffusion of Mn into GaAs, resulting in improved spin injection properties compared with those for a Co_2MnSi/*n*-GaAs junction. © *2014 AIP Publishing LLC*. [http://dx.doi.org/10.1063/1.4873720]

Electrical injection and detection of spin-polarized electrons using ferromagnet/semiconductor heterojunctions are a major prerequisite for creating viable semiconductor spintronic devices. There have been several reports on electrical spin injection and detection through the observation of spin-valve signals and Hanle signals in a four-terminal nonlocal geometry.[1–10] A highly polarized spin source is indispensable for efficient spin injection and detection. Co-based Heusler alloys are one candidate for a highly polarized spin source, because some of them are theoretically predicted to be half-metallic,[11,12] and they have high Curie temperatures that are well above room temperature. These alloys have been extensively applied to spintronic devices, including magnetic tunnel junctions (MTJs)[13–18] and giant magnetoresistance (GMR) devices.[19–23] We recently demonstrated high tunnel magnetoresistance (TMR) ratios of up to 1995% at 4.2 K and up to 354% at 290 K in Co_2MnSi/MgO/Co_2MnSi MTJs with Mn-rich Co_2MnSi electrodes.[18] The observed high TMR ratios for MTJs with Mn-rich Co_2MnSi electrodes are attributed to suppressed Co_{Mn} antisites, which leads to the enhanced half-metallicity through a reduced density of minority-spin in-gap states around E_F.[24,25] Furthermore, we reported relatively high TMR ratios of 448% at 300 K and 1113% at 4.2 K in an MTJ with a Co_2MnSi upper electrode via an ultra-thin CoFe insertion layer on a MgO tunnel barrier—i.e., a Co_2MnSi upper electrode/CoFe insertion layer/MgO barrier/CoFe lower electrode MTJ[26]—indicating a high spin polarization for Co_2MnSi.

In contrast, the feasibility of Co-based Heusler alloys as a half-metallic spin source for spin injection into semiconductors has not been fully clarified, and there have been very few reports on electrical detection of the spin injection using Co-based Heusler alloy electrodes.[5–7] Recently, we demonstrated a higher spin injection efficiency in Co_2MnSi/CoFe (1.1 nm)/*n*-GaAs junctions which exceeded that in CoFe (5.0 nm)/*n*-GaAs junctions, indicating a high spin polarization arising from the half-metallic character for Co_2MnSi.[5] However, the role of the CoFe insertion layer has not been clarified in detail. The optimal CoFe thickness is also unknown. The purpose of the present study is to elucidate the effect of a CoFe insertion layer on the spin injection properties in Co_2MnSi/CoFe/*n*-GaAs Schottky tunnel junctions. To do this, we systematically investigate the CoFe thickness dependence of the spin injection efficiency for Co_2MnSi/CoFe (0 – 4.1 nm)/*n*-GaAs Schottky tunnel junctions which are fabricated in one GaAs substrate. We also investigate the degree of diffusion for atomic species at Co_2MnSi/*n*-GaAs interfaces with and without a CoFe insertion layer by secondary ion mass spectrometry (SIMS) analysis and discuss the effect of a CoFe insertion layer.

A layer structure consisting of (from the substrate side) a 250-nm-thick undoped GaAs buffer layer, a 2500-nm-thick n^--GaAs ($Si = 3 \times 10^{16}\,cm^{-3}$) channel layer, and a 30-nm-thick n^+-GaAs ($Si = 5 \times 10^{18}\,cm^{-3}$) highly doped layer was grown by molecular beam epitaxy at 600 °C on a semi-insulating GaAs (001) substrate (Fig. 1(a)). This layer structure is similar to that reported in Ref. 4. The sample was then capped with an arsenic protective layer and transported to a magnetron sputtering chamber. After the arsenic cap was removed by heating the sample to 400 °C, a CoFe insertion layer having a wedge-shaped structure whose thickness (t_{CoFe}) ranged from 0 to 4.1 nm and a 5-nm-thick $Co_2Mn_{1.30}Si_{0.84}$ (CMS) spin source layer was then deposited on GaAs by magnetron sputtering at room temperature and successively annealed *in situ* at 400 °C. A Mn-rich CMS film of $Co_2Mn_{1.30}Si_{0.84}$ was used to suppress the harmful Co_{Mn} antisite to improve the half-metallicity.[24,25] Finally, a 5-nm-thick Ru cap layer was deposited using magnetron sputtering at room temperature. Figure 1(b) shows a high-angle annular dark-field scanning transmission electron microscope (HAADF STEM) image of a layer structure of Ru/Co_2MnSi/CoFe (1.3 nm)/GaAs(001). An atomically flat and abrupt interface facing GaAs was formed. Using electron beam lithography and Ar ion milling techniques, lateral spin-transport devices as shown in Fig. 1(c) were fabricated. The size of the injector contact (contact-2) and detector contact (contact-3) were

a)E-mail: uemura@ist.hokudai.ac.jp

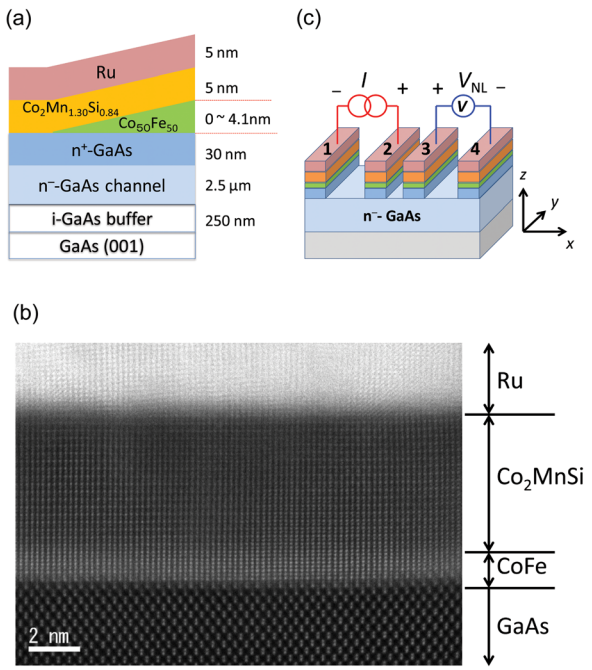

FIG. 1. (a) Schematic diagram of layer structure. (b) HAADF STEM image of a layer structure of Ru/Co_2MnSi/CoFe(1.3 nm)/GaAs(001). (c) Schematic diagram of lateral spin-transport device.

$0.5 \times 10\,\mu$m and $1.0 \times 10\,\mu$m, respectively, and the spacing between the contacts was $0.5\,\mu$m. The spin injection properties were evaluated in a four-terminal nonlocal geometry where the nonlocal voltage (V_{NL}) between contact-3 and contact-4 was measured under a constant current (I) supplied between contact-2 and contact-1 as functions of the in-plane magnetic field for spin-valve signal measurements and the out-of-plane magnetic field for Hanle effect measurements. The bias voltage was defined with respect to the n-GaAs.

As will be shown and discussed later, the spin injection efficiency strongly depended on t_{CoFe}, and it reached the maximum at $t_{CoFe} = 1.3$ nm. Figures 2(a) and 2(b) show a typical spin-valve signal and Hanle signal measured at 4.2 K for a CMS/CoFe (t_{CoFe})/n-GaAs junction with $t_{CoFe} = 1.3$ nm. The junction was positively biased with a supplied current $I = +10\,\mu$A, where electron spins were extracted from n-GaAs to CMS. An in-plane magnetic field (B_y) was applied along the longitudinal direction of the junction (the y axis direction). A clear spin-valve signal was observed due to switching between the parallel (P) and antiparallel (AP) states for the relative magnetization configuration between the injector and detector contacts at $B_y \cong +8$ and -8 mT. A nonlocal voltage change (ΔV_{NL}) of approximately 44 μV was obtained, where ΔV_{NL} is defined as $V_{NL}{}^{P} - V_{NL}{}^{AP}$, and where $V_{NL}{}^{P}$ and $V_{NL}{}^{AP}$ are nonlocal voltages for the P and AP configurations, respectively, between injector contact-2 and detector contact-3. Clear Hanle signals were also observed for both P and AP configurations, as shown in Fig. 2(b). Observation of both the spin-valve signal and the Hanle signals is strong evidence of injection, transport, and detection of spin-polarized electrons in the CMS/CoFe/n-GaAs lateral transport device. Based on the conventional spin diffusion model, the Hanle signal can be expressed by[27]

$$V_{NL}(B_z)/I = \pm\frac{P_{inj}P_{det}}{2}\left(\rho\frac{l_{sf}}{S}\right)\left(\frac{2l_{sf}}{\tau_s}\right)\int_0^\infty \frac{1}{\sqrt{4\pi Dt}}\exp \times\left(-\frac{d^2}{4Dt}\right)\cos\Omega_L(B_z)t\exp\left(-\frac{t}{\tau_s}\right)dt, \quad (1)$$

where B_z is an out-of-plane magnetic field, $P_{inj(det)}$ is the spin polarization of the injector (detector) contact, ρ is the resistivity of the GaAs channel, S is the area of the channel cross-section, l_{sf} is the spin-diffusion length, d is the distance between contact-2 and contact-3, τ_s is the spin lifetime, I is the injection current, $D = l_{sf}{}^2/\tau_s$ is the diffusion constant, $\Omega_L(B_z) = g\mu_B B_z/\hbar$ is the Larmor frequency, g is an electron g factor in the channel ($g = -0.44$ for GaAs), μ_B is the Bohr magneton, and $\hbar$ is the reduced Planck's constant. The sign of $+$ ($-$) on the right-hand side of Eq. (1) corresponds to the P (AP) configuration. The observed Hanle curve can be fitted well with Eq. (1). The estimated values of τ_s and l_{sf} from fitting were 20 ns and 3 μm, respectively. These values are comparable to those observed for a CoFe (5 nm)/n-GaAs sample with an identical channel structure.[4] On the other hand, the effective spin polarization defined by $(P_{inj}P_{det})^{1/2}$ was 0.52, a value almost 13 times larger than that for the CoFe/n-GaAs sample.

Here, we introduce $\Delta V_{NL}/I$ as a measure of spin injection efficiency, because it is proportional to $P_{inj}P_{det}$ from Eq. (1). Figure 3(a) shows the bias-current dependence of

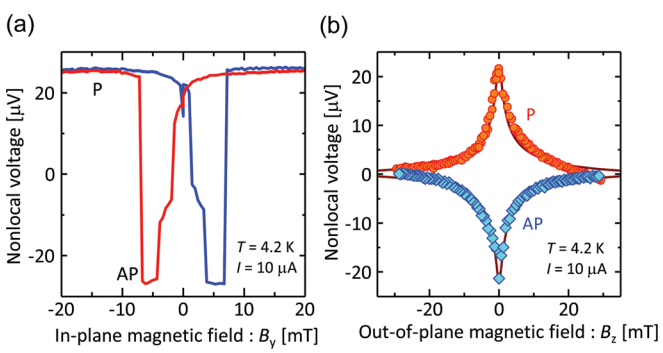

FIG. 2. (a) Typical spin-valve signal and (b) Hanle signal in a nonlocal geometry for a Co_2MnSi/CoFe (1.3 nm)/n-GaAs junction at 4.2 K.

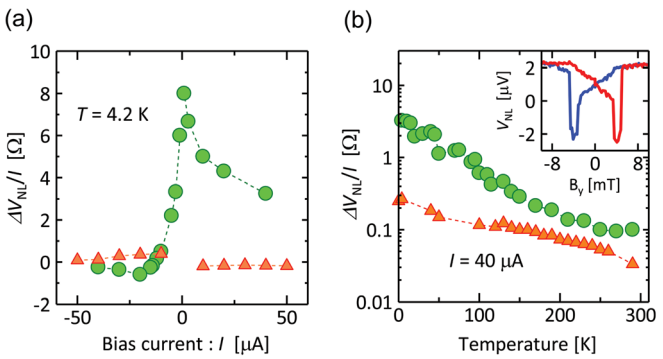

FIG. 3. (a) Bias-current dependence and (b) temperature dependence of $\Delta V_{NL}/I$ in spin-valve signals for a Co_2MnSi/CoFe (1.3 nm)/n-GaAs junction (circle) and a CoFe/n-GaAs junction (triangle). The inset of Fig. 3(b) shows a spin-valve signal for the Co_2MnSi/CoFe (1.3 nm)/n-GaAs junction at 290 K.

$\Delta V_{NL}/I$ at 4.2 K for a CMS/CoFe (1.3 nm)/*n*-GaAs junction and a CoFe (5 nm)/*n*-GaAs junction. The $\Delta V_{NL}/I$ values for the CMS/CoFe (1.3 nm)/*n*-GaAs junction decreased as $|I|$ increased, and the sign of $\Delta V_{NL}/I$ changed at $I \approx -14\ \mu$A. This indicates that the magnitude and sign of $P_{inj}P_{det}$ strongly depends on the bias condition. Although there have been several experimental[1,3–5] and theoretical[28–30] investigations into whether the magnitude and sign of the spin polarization for a ferromagnet/GaAs heterojunction are affected by the bias condition, the origin is still an open question and is beyond the scope of this paper. Importantly, the absolute values of $\Delta V_{NL}/I$ for the CMS/CoFe (1.3 nm)/*n*-GaAs junction were much higher than those of the CoFe/*n*-GaAs junction for almost all the bias region. In particular, the maximum value ($\sim$8 Ω) was one order of magnitude higher than that of CoFe/*n*-GaAs. Thus, CMS works as a highly polarized spin source in the CMS/CoFe (1.3 nm)/*n*-GaAs junction even though a 1.3-nm-thick CoFe layer was inserted between the CMS and GaAs. Figure 3(b) shows $\Delta V_{NL}/I$ for the CMS/CoFe (1.3 nm)/*n*-GaAs junction and the CoFe (5 nm)/*n*-GaAs junction as a function of temperature (T) from 4.2 K to 290 K. As shown in the inset of Fig. 3(b), a clear spin-valve signal was observed even at 290 K. Although the T dependence of $\Delta V_{NL}/I$ for the CMS/CoFe/*n*-GaAs junction is slightly stronger than that for the CoFe/*n*-GaAs junction, the value of $\Delta V_{NL}/I$ is still larger even at 290 K. It is noteworthy that the $\Delta V_{NL}/I$ of 0.1 Ω at 290 K obtained for the CMS/CoFe/*n*-GaAs junction is the highest yet reported for spin injections into GaAs or Si at room temperature.

Figures 4(a) and 4(b) show the t_{CoFe} dependence of $\Delta V_{NL}/I$ and the resistance-area product (RA) for CMS/CoFe(t_{CoFe})/*n*-GaAs junctions at 4.2 K. The resistance values were evaluated as $R = (dI/dV|_{V=0})^{-1}$, where I is a current flowing through the junction and V is a voltage across the junction. The $\Delta V_{NL}/I$ values strongly depended on t_{CoFe}. At $t_{CoFe} = 0$—i.e., for the CMS/*n*-GaAs junction—no clear spin signal was observed. The value of $\Delta V_{NL}/I$ increased as t_{CoFe} increased and reached the maximum value of approximately 8 Ω at $t_{CoFe} = 1.3$ nm. It then rapidly decreased as t_{CoFe} increased further, and it reached to 0.2 Ω at $t_{CoFe} = 4.1$ nm, a value comparable to that for the CoFe (5 nm)/*n*-GaAs sample. The RA values, on the other hand, decreased almost monotonically as t_{CoFe} increased. However, since the junction resistance for all devices is at least two orders of magnitude higher than the spin resistance, $\rho l_{sf}/S$, of the GaAs channel, all the devices investigated in this study were free from the impedance-mismatching problem, and $\Delta V_{NL}/I$ values do not depend on RA.[31] Thus, the difference in $\Delta V_{NL}/I$ values does not originate from the difference in RA, but from the difference in $P_{inj} \cdot P_{det}$.

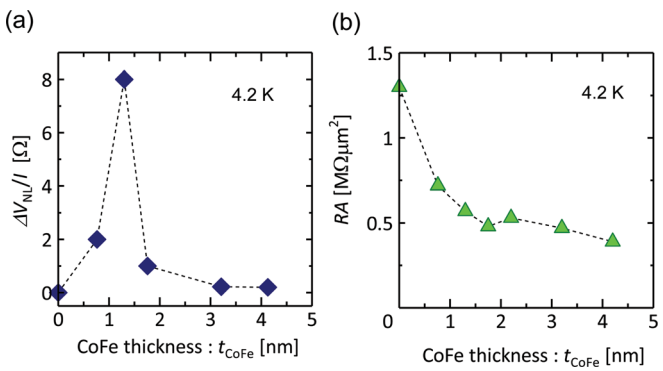

FIG. 4. CoFe thickness (t_{CoFe}) dependence of (a) $\Delta V_{NL}/I$ and (b) RA for Co_2MnSi/CoFe(t_{CoFe})/*n*-GaAs junctions at 4.2 K.

Now we will discuss the effect of CoFe insertion on the spin injection properties. One possible origin of the deterioration in the spin injection properties of the CMS/*n*-GaAs junction compared with junctions having an ultra-thin CoFe insertion layer is lower crystal quality of the CMS directly grown on GaAs. The reflection high energy electron diffraction (RHEED) observation of the CMS film grown on CoFe/*n*-GaAs showed a clear streak pattern, while that of the CMS film directly grown on GaAs showed no streak pattern before annealing (*not shown*). This indicates that the insertion of CoFe improves the crystal quality of the CMS. However, after annealing of the sample at 400 °C, the RHEED pattern of the CMS grown on GaAs also became streaky, and no clear difference was seen between the RHEED patterns, indicating the crystal quality of the CMS film grown on GaAs became comparable to that grown on CoFe/GaAs. Another possible origin of the deterioration in spin injection properties is diffusion of atomic species at the interface during the post-deposition annealing. To investigate the atomic diffusion at the interface, we did SIMS measurements for Co, Mn, Si, Fe, Ga, and As atoms at different positions for $t_{CoFe} = 0$ and 1.3 nm. As shown in Fig. 5, significant Mn diffusion into GaAs occurred for the CMS/*n*-GaAs junction compared to the CMS/CoFe (1.3 nm)/*n*-GaAs. On the other hand, no clear differences were seen for other atoms between the two samples (*not shown*). These results indicate that the diffusion of Mn degrades the spin injection properties of the CMS/*n*-GaAs. This is reasonable, because diffused Mn atoms may work as magnetic impurities which destroy the spin states of the electrons injected into GaAs.

Thus, the increase of spin injection signals up to $t_{CoFe} = 1.3$ nm was mainly due to the suppression of Mn atom diffusion. On the other hand, the reduction of spin

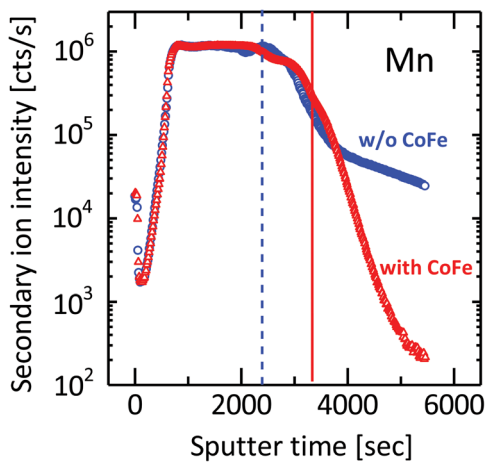

FIG. 5. Result of SIMS analysis for Co_2MnSi/CoFe (1.3 nm)/*n*-GaAs (red triangle) and Co_2MnSi/*n*-GaAs junctions (blue circle). The solid line and broken line indicate the interfaces facing GaAs for Co_2MnSi/CoFe (1.3 nm)/*n*-GaAs and Co_2MnSi/*n*-GaAs, respectively. The right side of each line corresponds to the *n*-GaAs region. There is a difference in the sputtering time needed to reach the GaAs surface between two samples with or without a CoFe insertion layer.

injection signals as t_{CoFe} increased at $t_{CoFe} > 1.3$ nm was possibly due to the reduction of spin polarization at the interface facing GaAs, because CoFe, whose spin polarization is smaller than that of CMS, works as a spin source as t_{CoFe} increases beyond 1.3 nm.

In summary, we investigated the CoFe thickness dependence of the spin injection efficiency for CMS/CoFe (t_{CoFe})/*n*-GaAs junctions, and experimentally found that the insertion of an ultrathin CoFe layer of ~1.3 nm between CMS and GaAs enables the suppression of Mn atom diffusion into GaAs and improved crystal quality along with high spin polarization at the interface facing GaAs, leading to a higher spin injection signal than that for CoFe/*n*-GaAs at both 4.2 K and 290 K. These results indicate that the insertion of an ultra-thin CoFe layer is a highly effective way to utilize the intrinsically high spin polarization of Co_2MnSi.

This work was partly supported by a Grant-in-Aid for Scientific Research (JSPS KAKENHI Grant No. 25286039), by the Murata Science Foundation, and by the Japan Science and Technology (JST) Agency through its Strategic International Cooperative Program under the title "Advanced spintronic materials and transport phenomena (ASPIMATT)." T.A. was also supported by a Research Fellowship for Young Scientists from the JSPS.

[1]X. Lou, C. Adelmann, S. A. Crooker, E. S. Garlid, J. Zhang, K. S. M. Reddy, S. D. Flexner, C. J. Palmstrøm, and P. A. Crowell, Nat. Phys. **3**, 197 (2007).
[2]M. Ciorga, A. Einwanger, U. Wurstbauer, D. Schuh, W. Wegscheider, and D. Weiss, Phys. Rev. B **79**, 165321 (2009).
[3]G. Salis, A. Fuhrer, R. R. Schlitter, L. Gross, and S. F. Alvarado, Phys. Rev. B **81**, 205323 (2010).
[4]T. Uemura, T. Akiho, M. Harada, K.-i. Matsuda, and M. Yamamoto, Appl. Phys. Lett. **99**, 082108 (2011).
[5]T. Akiho, J. Shan, H.-x. Liu, K.-i. Matsuda, M. Yamamoto, and T. Uemura, Phys. Rev. B **87**, 235205 (2013).
[6]P. Bruski, Y. Manzke, R. Farshchi, O. Brandt, J. Herfort, and M. Ramsteiner, Appl. Phys. Lett. **103**, 052406 (2013).
[7]T. Saito, N. Tezuka, M. Matsuura, and S. Sugimoto, Appl. Phys. Express **6**, 103006 (2013).
[8]T. Sasaki, T. Oikawa, T. Suzuki, M. Shiraishi, Y. Suzuki, and K. Noguchi, IEEE Trans. Magn. **46**, 1436 (2010).
[9]Y. Saito, M. Ishikawa, T. Inokuchi, H. Sugiyama, T. Tanamoto, K. Hamaya, and N. Tezuka, IEEE Trans. Magn. **48**, 2739 (2012).
[10]Y. Zhou, W. Han, L.-T. Chang, F. Xiu, M. Wang, M. Oehme, I. A. Fischer, J. Schulze, R. K. Kawakami, and K. L. Wang, Phys. Rev. B **84**, 125323 (2011).
[11]S. Ishida, S. Fujii, S. Kashiwagi, and S. Asano, J. Phys. Soc. Jpn. **64**, 2152 (1995).
[12]S. Picozzi, A. Continenza, and A. J. Freeman, Phys. Rev. B **66**, 094421 (2002).
[13]S. Kämmerer, A. Thomas, A. Hütten, and G. Reiss, Appl. Phys. Lett. **85**, 79 (2004).
[14]Y. Sakuraba, M. Hattori, M. Oogane, Y. Ando, H. Kato, A. Sakuma, T. Miyazaki, and H. Kubota, Appl. Phys. Lett. **88**, 192508 (2006).
[15]T. Ishikawa, T. Marukame, H. Kijima, K.-i. Matsuda, T. Uemura, M. Arita, and M. Yamamoto, Appl. Phys. Lett. **89**, 192505 (2006).
[16]N. Tezuka, N. Ikeda, F. Mitsuhashi, and S. Sugimoto, Appl. Phys. Lett. **94**, 162504 (2009).
[17]T. Ishikawa, H.-x. Liu, T. Taira, K.-i. Matsuda, T. Uemura, and M. Yamamoto, Appl. Phys. Lett. **95**, 232512 (2009).
[18]H.-x. Liu, Y. Honda, T. Taira, K.-i. Matsuda, M. Arita, T. Uemura, and M. Yamamoto, Appl. Phys. Lett. **101**, 132418 (2012).
[19]K. Yakushiji, K. Saito, S. Mitani, K. Takanashi, Y. K. Takahashi, and K. Hono, Appl. Phys. Lett. **88**, 222504 (2006).
[20]T. Furubayashi, K. Kodama, H. Sukegawa, Y. K. Takahashi, K. Inomata, and K. Hono, Appl. Phys. Lett. **93**, 122507 (2008).
[21]Y. Sakuraba, K. Izumi, T. Iwase, S. Bosu, K. Saito, K. Takanashi, Y. Miura, K. Futatsukawa, K. Abe, and M. Shirai, Phys. Rev. B **82**, 094444 (2010).
[22]J. Sato, M. Oogane, H. Naganuma, and Y. Ando, Appl. Phys. Express **4**, 113005 (2011).
[23]M. J. Carey, S. Maat, S. Chandrashekariaih, J. A. Katine, W. Chen, B. York, and J. R. Childress, J. Appl. Phys. **109**, 093912 (2011).
[24]M. Yamamoto, T. Ishikawa, T. Taira, G.-f. Li, K.-i. Matsuda, and T. Uemura, J. Phys.: Condens. Matter **22**, 164212 (2010).
[25]G.-f. Li, Y. Honda, H.-x. Liu, K.-i. Matsuda, M. Arita, T. Uemura, M. Yamamoto, Y. Miura, M. Shirai, T. Saito, F. Shi, and P. M. Voyles, Phys. Rev. B **89**, 014428 (2014).
[26]H.-x. Liu, T. Taira, Y. Honda, K.-i. Matsuda, T. Uemura, and M. Yamamoto, 55th Annual Conf. on Magnetism & Magnetic Materials, Atlanta, Georgia, USA, 370 (2010).
[27]J. Fabian, A. Matos-Abiaguea, C. Ertler, P. Stano, and I. Žutić, Acta Phys. Slovaca **57**, 565 (2007).
[28]H. Dery and L. J. Sham, Phys. Rev. Lett. **98**, 046602 (2007).
[29]A. N. Chantis, K. D. Belashchenko, D. L. Smith, E. Y. Tsymbal, M. van Schilfgaarde, and R. C. Albers, Phys. Rev. Lett. **99**, 196603 (2007).
[30]S. Honda, H. Itoh, and J. Inoue, J. Phys. D: Appl. Phys. **43**, 135002 (2010).
[31]A. Fert and H. Jaffrès, Phys. Rev. B **64**, 184420 (2001).